

# Investigation on mass diffusion process in porous media based on Lattice Boltzmann method

Y. M. Xuan · K. Zhao · Q. Li

Received: 11 May 2010 / Accepted: 8 September 2010 / Published online: 24 September 2010  
© Springer-Verlag 2010

**Abstract** The mass diffusion process inside a porous medium is difficult for numerical simulation due to complex and stochastic nature of its structure. Based on the lattice Boltzmann method and reconstruction technology, this article presents an approach for simulating mass diffusion process and predicting the effective mass diffusivity in porous media, which is validated by comparing theoretical and experimental data. The concentration distribution and effective mass diffusivity inside porous media can be obtained.

## 1 Introduction

Different types of transport phenomena in porous media play important roles in many fields such as petroleum engineering, medicinal materials, agricultural and building materials. For better understanding of transport mechanism in these fields, the macroscopic effective transport properties of a porous medium such as permeability, conductivity and mass diffusivity have been studied for well over 100 years in both theory and experiment. There have been many previous works about the heat and fluid flow inside a porous medium [1–8], but few ones up to now are about the mass diffusion process.

Recently, it is found that many building materials of micro-porous structures emit volatile organic compounds

(VOCs), which may cause sick building syndrome (SBS) such as headache, eye irritation, nose or throat irritation, dry cough, dizziness and nausea, even difficulty in concentrating and tiredness. For the purpose of establishing friendly inhabitation, there has been growing interest in studying mass transfer process inside building materials which in fact are porous medium [9–11]. The effective mass diffusivity is one of the most important parameters characterizing the mass transport properties of a porous medium and has been studied extensively by using both theoretical and experimental approaches [12–17]. In the former, the theoretical models are mainly proposed based on the continuous governing equations at the representative elementary volume (REV) scale and the physical parameters, especially diffusion coefficients involved in the equations are usually obtained from experiment data or some empirical equations. Most of these models ignore the influence of the microstructures inside the porous medium and therefore have some intrinsic limitations because the microscopic feature may be very important for getting insight into the heat and mass transfer in porous media. Although the experimental data are valuable, it is difficult to apply these results obtained from the test conditions to those corresponding to other practical conditions and can hardly reveal the transport mechanism in complex structures. To our knowledge up to now, investigation efforts on direct simulation of the mass diffusion inside porous media at pore scale and theoretical prediction of the effective mass diffusivity of fluid or components inside porous media without resorting to any experiment or empirical parameters have appeared to be little.

The objective of this work is to develop a comprehensive approach for the theoretical prediction of the effective mass diffusivities of fluids inside porous media based on analysis of mass transfer process at the pore scale of the

---

Dedicated to Professor Dr. Ing. Dr. h.c. mult. Karl Stephan on the occasion of his 80th birthday.

---

Y. M. Xuan (✉) · K. Zhao · Q. Li  
School of Power Engineering, Nanjing University of Science and Technology, Nanjing 210094, People's Republic of China  
e-mail: ymxuan@mail.njust.edu.cn

porous media. With this approach, one can calculate the effective mass diffusivities and investigate the mass transfer process inside a variety of porous media such as regular or random two- and three-dimensional porous media at the pore scale. This approach is fully theoretical without resorting to any empirical parameters of accounting for the possible effects of different factors on the mass diffusion process inside porous media. For such purpose, we will apply the lattice Boltzmann method to simulate mass diffusion inside a porous medium by means of a spatially varying relaxation time. Some types of “digital porous media” are constructed with the reconstruction technology for two- and three-dimensional porous media. This theoretical approach will be validated by means of some benchmark examples. Furthermore, comparison between the presented approach and some existing equations such as Maxwell equation and Nield equation is conducted. The effect of random structure of porous media on the mass transport process is discussed to reveal difference between regular and random porous media. The influence of the average granular diameter on the effective mass diffusivity is also investigated. The work of this paper provides a approach for mechanism analysis of mass diffusion processes inside porous media such as the VOCs problem.

## 2 Numerical method

### 2.1 Governing equation

The mass diffusion equation without homogeneous chemical reactions is [18]

$$\frac{\partial C}{\partial t} = D \nabla^2 C \quad (1)$$

where  $C$  is molar concentration,  $D$  is mass diffusion coefficient (i.e., mass diffusivity).

### 2.2 Lattice Boltzmann method

The lattice Boltzmann method (LBM) is intrinsically a mesoscopic approach based on the evolution of statistical distribution on lattices, which originates from the kinetic Boltzmann equation and becomes popular over the past few years. This method treats a fluid as an ensemble of artificial particles and explores the microscopic features of the fluid by using the collision effect among these particles. It is proved that the lattice BGK method is consistent with the Navier–Stokes equation for fluid flow through Chapman–Enskog expansion [19]. This method bridges the gap between the microscopic world and the macroscopic phenomena. It has attracted more and more attentions in

simulating fluid flows and thermal processes as well as associated transport phenomena. The most important advantages of LBM are the easy implementation of multiple interparticle interactions and complex geometry boundary conditions [19–23].

As a novel numerical approach, the lattice Boltzmann method is introduced to investigate the diffusion mass transfer process inside porous media in this paper. Generally, the discretized Boltzmann evolution equation without any external force term is expressed as

$$f_x(\mathbf{x} + \mathbf{e}_x \delta t, t + \delta t) - f_x(\mathbf{x}, t) = -\frac{1}{\tau} (f_x(\mathbf{x}, t) - f_x^{eq}(\mathbf{x}, t)) \quad (2)$$

where  $f_x$  is the particle distribution function,  $\delta t$  is the time step,  $\tau$  is the non-dimensional relaxation time,  $\mathbf{e}_x$  is the discrete lattice velocity, and subscript  $\alpha = 0, 1, 2, \dots, b$  is for the velocity direction. The lattice velocities may have different forms corresponding to the lattice structure of the LB model such as D2Q9, D3Q7 and D3Q15.

For mass diffusion equation, the equilibrium distribution function is expressed as [24]

$$f_x^{eq}(\mathbf{x}, t) = \frac{C}{(b+1)} \quad (3)$$

where the concentration  $C$  is given as

$$C = \sum_{\alpha} f_{\alpha} \quad (4)$$

and  $(b+1)$  is the number of the discrete lattice velocities.

Keep in mind that Eq. 1 is a pure diffusive equation without containing convective term, it has been known that 90° rotational invariance of lattices is sufficient to yield full isotropy for pure diffusive phenomena and a square or a cubic lattice in two or three dimensions is enough, respectively, without degrading the accuracy [25]. Thus, the D2Q5 square lattice and D3Q7 cubic lattice LBM models shown in Fig. 1 are introduced for 2D and 3D simulations, respectively.

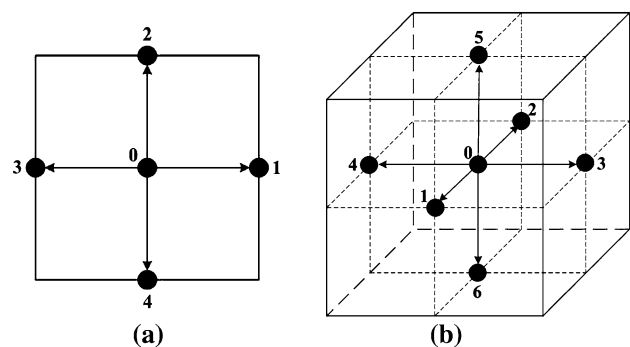


**Fig. 1** Schematic of the velocity directions for the D2Q5 and D3Q7 models. **a** D2Q5 model, **b** D3Q7 model

For 2D cases, the discrete velocities of D2Q5 model become

$$\mathbf{e}_x = \begin{bmatrix} 0 & c & 0 & -c & 0 \\ 0 & 0 & c & 0 & -c \end{bmatrix}. \quad (5)$$

For 3D cases, the discrete velocities of D3Q7 model are given by

$$\mathbf{e}_x = \begin{bmatrix} 0 & c & -c & 0 & 0 & 0 & 0 \\ 0 & 0 & 0 & c & -c & 0 & 0 \\ 0 & 0 & 0 & 0 & 0 & c & -c \end{bmatrix} \quad (6)$$

where  $c$  is a lattice speed, defined as  $\delta_x/\delta_t$ , where  $\delta_x$  is a lattice constant (i.e., the grid size), whose value can only take any positive number to insure  $\tau$  to be within (0.5, 2) [26, 27]. A larger  $c$  may result in a more accurate concentration prediction near the boundaries but with higher computational costs.

In order to ensure convergence of the solution of the lattice Boltzmann model to that diffusion Eq. 1, the following relations between the macroscopic parameter (i.e., mass diffusivity) and the microscopic non-dimensional relaxation time are obtained through Chapman-Enskog expansion.

For D2Q5 model, the relation is

$$D = \frac{2}{5}c^2(\tau - 0.5)\delta t. \quad (7)$$

For D3Q7 model, the relation is

$$D = \frac{2}{7}c^2(\tau - 0.5)\delta t. \quad (8)$$

### 3 Mass diffusion in porous media

The above-mentioned LB model is for a mass diffusion problem inside homogeneous media (without solid matrix). But for the mass diffusion process in a porous medium, the pore structure and zigzag channel in the porous medium make the mass diffusion more complicated. The known structure feature is prerequisite for treating the mass diffusion problem in the porous medium. The digital reconstruction or imaging of a real porous medium is necessary for numerical computation of mass transfer process in the porous medium.

#### 3.1 Reconstruction of porous media and mesh size

In order to investigate the mass diffusion process inside a porous medium with the LBM at pore scale, one should reconstruct porous media such as simple regular structure, two- or three-dimensional random porous media for the purpose of numerical computation.

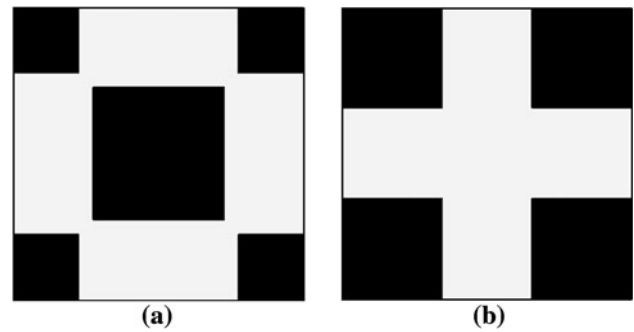


**Fig. 2** Calculation regular structures for the 2D case. **a** Staggered square grains, **b** in-line square grains

#### 3.1.1 Regular structure

For the sake of simplicity, the two-dimensional regular porous media with square grains for both staggered and in-line arrangements are first considered (as shown in Fig. 2). With these simple structures, it may be a good test for this present method to reveal some basic mechanism for the mass diffusion inside porous media. Taking the geometric periodicity into account, it is enough to consider a single periodic module with the dimension of  $L \times L$ . By considering the computational time and the precision, the domain of  $L \times L$  is divided into  $201 \times 201$  for 2D case.

#### 3.1.2 Random structure

To our best knowledge, most of real porous media in nature have inherent random geometric properties such as grain or pore shape and the random volumetric and topological properties such as pore tortuosity and interconnectivity, which are very important for describing the mass diffusion process inside porous media. The quartet structure generation set (QSGS) proposed by Wang and Chen [28] is introduced to reconstruct random granular porous media with various parameters such as porosity and particle diameter, which is applicable and versatile for theoretical investigation. Figure 3 shows the reconstructed random porous media using our two- and three-dimensional QSGS codes. In Fig. 3,  $\phi$  is defined as the granular fraction (i.e., solid matrix fraction) and the whole domain  $L \times L \times L$  is set to be  $60 \times 60 \times 60$ .

#### 3.2 Governing equation for the mass diffusion problem inside porous media

Consider a porous medium with either permeable or non-permeable inclusions imposed with a constant concentration gradient as shown in Fig. 4, the mass transfer process can be locally described by the following mass diffusion equation [29]

**Fig. 3** Calculation random structures. **a** Two-dimensional ( $\phi = 0.3$ ), **b** two-dimensional ( $\phi = 0.6$ ), **c** three-dimensional ( $\phi = 0.3$ ), **d** three-dimensional ( $\phi = 0.6$ )

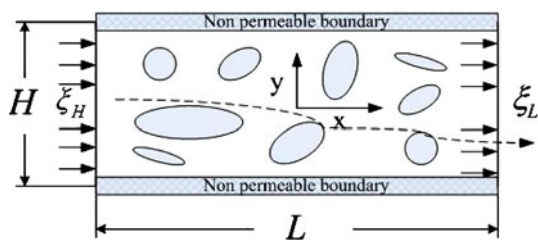
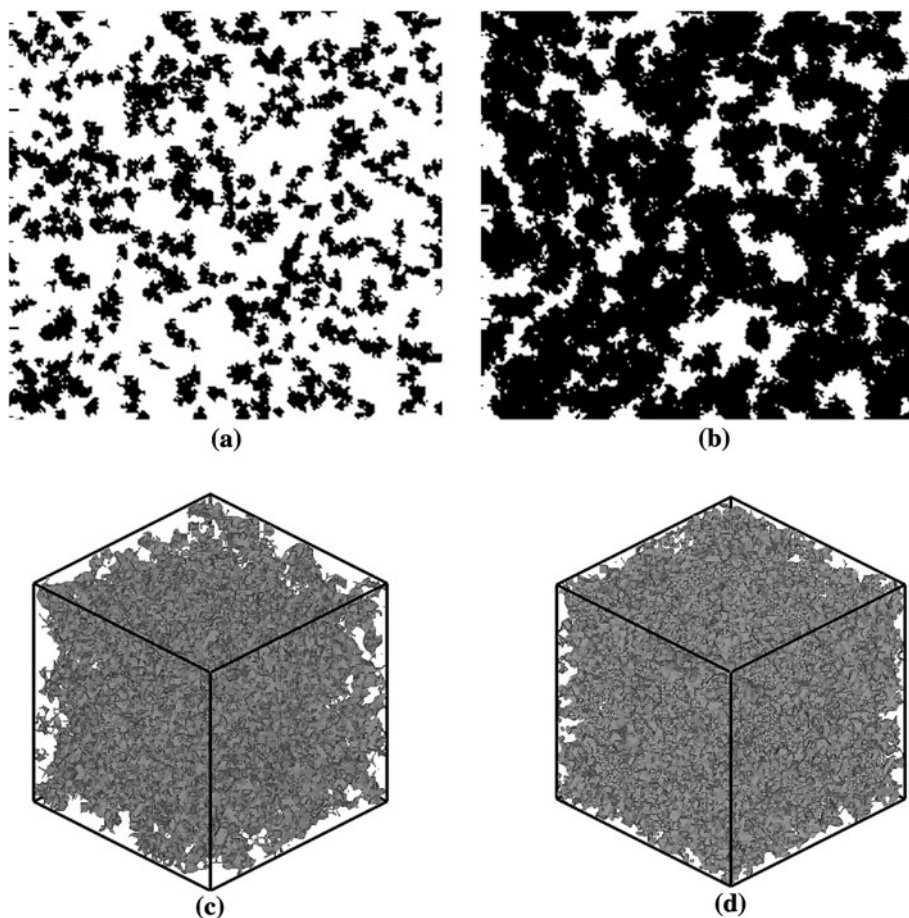


**Fig. 4** Schematic for prediction of effective mass diffusivity

$$\frac{\partial \chi}{\partial t} = D_p \nabla^2 \chi \tag{9}$$

where  $\chi$  is the local molar concentration, and  $D_p$  is the local molecular diffusivity being equal to  $D_C$  in the pore phase and  $D_I$  in the solid phase.

Generally, the average pore size is much smaller than the typical length scale involved in describing the mass diffusion problem. Hence, the mass transport in the whole domain may be rewritten as the macroscopic diffusion equation

$$\frac{\partial C}{\partial t} = D_{eff} \nabla^2 C \tag{10}$$

where  $C$  is the macroscopic mean concentration and  $D_{eff}$  is the effective mass diffusivity along the  $x$  direction. The effective mass diffusivity is defined as follows:

$$D_{eff} = \frac{w^*}{w} D_C \tag{11}$$

where the parameter  $w$  and  $w^*$  are for the steady-state molar flux across the homogeneous media (without solid matrix) and the steady-state molar flux across the heterogeneous media (with solid matrix), respectively. They are expressed as follows

$$w = D_C (\xi_H - \xi_L) L_2 / L_1 \tag{12}$$

$$w^* = \int_0^{L_2} D_p (\partial \xi / \partial x)_{x=L_1} dy \tag{13}$$

There are two analytic approaches proposed by Maxwell and Nield to predict the effective diffusion parameters (such as mass diffusivity or thermal conductivity) to account for the effect of inclusions in media, which are given by the following expressions [30, 31].

Maxwell equation:

$$\frac{D_{eff}}{D_C} = \frac{2D_C + D_I - 2\phi(D_C - D_I)}{2D_C + D_I + \phi(D_C - D_I)} \tag{14}$$

Nield equation:

$$\frac{D_{eff}}{D_C} = \left( \frac{D_I}{D_C} \right)^\phi. \quad (15)$$

### 3.3 Special treatment for the solid matrix

#### 3.3.1 Permeable solid matrix

The permeability of grains is very important to the mechanism of the effective mass diffusion and dispersion inside porous media. If the grains are permeable, the mass species may diffuse not only along the pores but also through the grains, which simultaneously cause variation of the apparent mass diffusivity of a whole porous medium. This phenomenon exists in some practical applications such as the surface diffusion for VOCs problem (i.e., the diffusion coefficient of VOCs within solid matrix). It is meaningful to investigate this phenomenon in which grains are treated as another permeable phase with different diffusivity.

In this paper the two different diffusivities of the species in pores and grains are determined by means of a spatially varying relaxation time in the lattice Boltzmann model according to Eqs. 7 or 8. This treatment is simple and intuitive and can be conveniently extended to three phase or more phase medium problems. Thus, the relationships between the two different types of mass diffusivities and the microscopic non-dimensional relaxation time are as follows.

For D2Q5 model, the relation is

$$D_C = \frac{2}{5}c^2(\tau_C - 0.5)\delta t, \quad D_I = \frac{2}{5}c^2(\tau_I - 0.5)\delta t. \quad (16)$$

For D3Q7 model, the relation is

$$D_C = \frac{2}{7}c^2(\tau_C - 0.5)\delta t, \quad D_I = \frac{2}{7}c^2(\tau_I - 0.5)\delta t \quad (17)$$

where  $\tau_C$  and  $\tau_I$  represents the non-dimensional relaxation time for mass diffusion process in pores and grains, respectively.

#### 3.3.2 Non-permeable solid matrix

If the grains are non-permeable, the species diffuse only along the pores. In such case, the area through which the species diffuse is much smaller than the one in the homogeneous media. Thus, the area change for diffusion causes variation of the mass diffusivity. In this case, we only need to use bounce-back scheme in the lattice Boltzmann model to deal with the solid–pore interfaces.

### 3.4 Boundary condition

Boundary conditions play important roles in lattice Boltzmann methods, which they will influence the accuracy and

stability of the LBM. Considering there are too many boundaries for the three-dimensional problem, for convenience, a universal boundary condition must be introduced here. Thus, we follow the nonequilibrium extrapolation rule proposed by Guo et al. [32], which is of second order and has better numerical stability

$$f_\alpha(\mathbf{x}_b, t) = f_\alpha^{eq}(\mathbf{x}_b, t) + f_\alpha^{neq}(\mathbf{x}_f, t) \quad (18)$$

where the subscripts  $b$  and  $f$  represent the node on the boundary and the nearest neighbour fluid node of  $\mathbf{x}_b$ , respectively. The nonequilibrium term  $f_\alpha^{neq}(\mathbf{x}_f, t)$  represents the deviation from the equilibrium, which is defined as

$$f_\alpha^{neq}(\mathbf{x}_f, t) = f_\alpha(\mathbf{x}_f, t) - f_\alpha^{eq}(\mathbf{x}_f, t). \quad (19)$$

Substituting Eq. 19 into Eq. 18, the particle distribution function on the boundary node can be given as

$$f_\alpha(\mathbf{x}_b, t) = f_\alpha^{eq}(\mathbf{x}_b, t) + f_\alpha(\mathbf{x}_f, t) - f_\alpha^{eq}(\mathbf{x}_f, t). \quad (20)$$

If the concentration on the boundary node  $xb$  is known, the equilibrium distribution function at the boundary  $f_\alpha^{eq}(\mathbf{x}_b, t)$  can be obtained easily by Eq. 3. Alternately, if the concentration gradient is known on the boundary node  $\mathbf{x}_b$ , an approximate concentration can be obtained by the Fick's law and then the treatment is the same as the specified concentration boundary.

### 3.5 Statistic of molar flux in a porous medium

The steady-state molar flux can be calculated using Eq. 13, but when considering the solid matrix in the medium, it is not very convenient. A simpler method is that the molar flux inside a porous medium can be obtained from the particle distribution function of LBM directly, where the volume thermal capacity  $\rho c_p$  is assumed to be 1 for the mass diffusion problem, according to our previous paper [33]. Thus, the statistical equation is defined as follows:

$$w^* = \sum_\alpha e_x f_\alpha \frac{\tau_p - 0.5}{\tau_p} \quad (21)$$

where  $\tau_p$  is the local non-dimensional relaxation time, which is equal to  $\tau_C$  in the pore phase and  $\tau_I$  in the solid phase.

## 4 Validation test

### 4.1 Existing theoretical solution for homogeneous media

To validate the procedure described in the previous section for LBM in a homogeneous media (without solid matrix), a diffusion problem in stationary media with specified



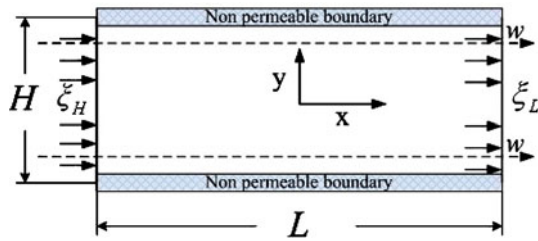


Fig. 5 Schematic of the problem

surface concentrations, shown in Fig. 5, is considered. The walls, located at  $y = 0$  and  $H$ , are non permeable boundary, the other ones, located at  $x = 0$  and  $L$ , are kept at constant concentrations,  $\xi_H$  and  $\xi_L$  ( $\xi_H > \xi_L$ ). In this case, the problem can be reduced to one-dimensional diffusion process, where there is a molar flux along the  $x$  direction because of the constant concentration gradient.

The governing equation for this case is Eq. 1. Without loss of generality, the dimensionless variables are used in this simulation and the characteristic parameters are listed in Table 1. Thus, the dimensionless governing equation for this case is

$$\frac{\partial \varphi}{\partial t^*} = Fo_m \nabla^{*2} \varphi \tag{22}$$

and the boundary conditions become

$$\begin{cases} \varphi = 1 & x^* = 0 \\ \varphi = 0 & x^* = 1 \end{cases} \tag{23}$$

where  $Fo_m = (Dt_0)/L^2$  is a dimensionless number.

The solution  $\varphi$  is given analytically by

$$\varphi = -x^* + 1. \tag{24}$$

For  $Fo_m = 4.0$ , calculations are carried out with  $41 \times 41$  and  $101 \times 101$  square grids. The lattice speed is fixed at 1,000. The convergent criteria is defined as

$$\frac{\sum_{ij} |\xi_{ij}^{n+1} - \xi_{ij}^n|}{\sum_{ij} |\xi_{ij}^{n+1}|} \leq 1.0 \times 10^{-9} \tag{25}$$

where  $\xi_{ij}^{n+1}$  is the concentration on the  $(i, j)$  node at the next time and  $\xi_{ij}^n$  is the one at the current time.

Figure 6 shows an excellent agreement with the analytical solution with two different grid resolutions and

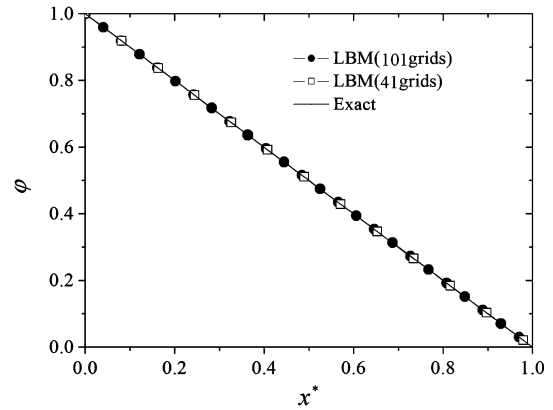


Fig. 6 Concentration profiles along the  $x$  direction

provides a good test of our lattice Boltzmann model with current boundary treatments.

#### 4.2 Experiment data for porous media

The existing theoretical solution for the diffusion problem in a porous medium can hardly be obtained. In order to validate our LBM for mass diffusion problem in a porous medium, some experiment data must be introduced. However, we can hardly find some better and simpler experiment results about the effective mass diffusivity in a porous medium in previous papers, fortunately, the results about the effective conductivity are reasonable and because of the similarity between the conduction equation and the mass diffusion equation, here, we can choose the effective conductivity as the experiment benchmark to test our diffusion LB model in porous media in this paper.

Figure 7 shows the two-dimensional porous structure truncated at two perpendicular cross directions of a polyurethane foam [34]. In each figure, the white part is the pore and the dark part represents the solid polyurethane. Measured data for this material are given in Ref. [34]. By the technology of the image analysis, these structures were transferred to  $242 \times 242$  pixels matrices and then used for simulations. The results listed in Table 2 show that

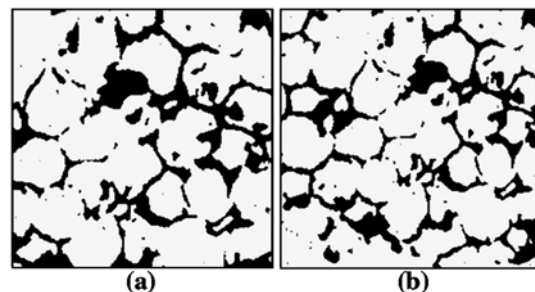


Fig. 7 Given structures of the polyurethane foam. **a** Along the foam growing direction, **b** across the foam growing direction

Table 1 Dimensionless variables and characteristic parameters

Variable	Characteristic parameters
Length: $x^* = x/L$	$L$
Concentration: $\varphi = (\xi - \xi_L)/(\xi_H - \xi_L)$	$(\xi_H - \xi_L)$
Time: $t^* = t/t_0$	$t_0$

**Table 2** Comparisons between present results and experimental data for given structures

Along the foam growing direction	
Prediction (W/mK)	0.0255
Experiment (W/mK)	0.0220
Deviation (%)	15.9
Across the foam growing direction	
Prediction (W/mK)	0.0286
Experiment (W/mK)	0.0245
Deviation (%)	9.3

the deviations of the predict effective conductivities are no  $>16\%$ , which is encouraging. It is expected that more finely matrices and improved experimental measurements would lead to closer agreements.

## 5 Results and discussion

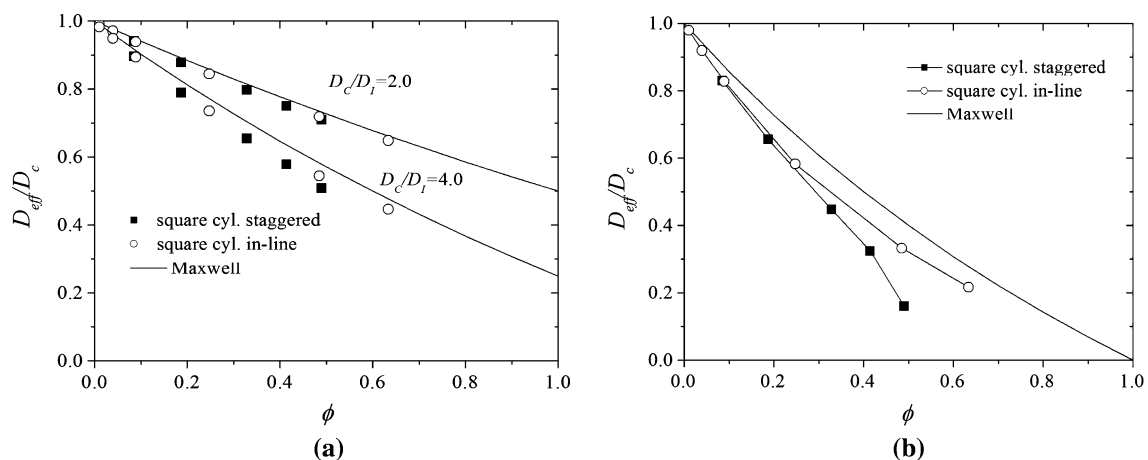
After validation by some theoretical solution and some experiment data, the proposed LBM is used to investigate mass diffusion process and predict the effective mass diffusivity in some complicate structures, such as 2D regular porous media, 2D or 3D random porous media. Furthermore, some meaningful results are obtained.

### 5.1 2D regular porous media

In 2D simulation, the effective mass diffusivity for regular porous structures consisting of either permeable or non-permeable grains are estimated and compared with the Maxwell equation. Calculations are carried out for species across a bank of square cylinders in staggered or in-line arrangement (see Fig. 2). Figure 8a shows the effective mass diffusivities for permeable grains versus the granular fraction.

The results for two values of  $D_c/D_l$ , namely 2.0 and 4.0 show that the effective mass diffusivities decrease with the grains fraction monotonically. The whole trends agree with the Maxwell equation. But the values for every granular fraction agree less favorably with it and the discrepancy increases with increasing  $D_c/D_l$ . For fixed  $D_c/D_l$ , the discrepancy increases with increasing  $\phi$  when the granular fraction is smaller than 0.5 and decreases when the granular fraction is larger than 0.5. This may be attributed to that when  $\phi$  is very small (close to 0), there are few grains in the domain and the influence of the granular shape or structure is very small, but when  $\phi$  increases ( $<0.5$ ), it may influence the predictions very much. When  $\phi$  is larger than 0.5, the whole domain is mainly occupied by solid matrix. Especially, when  $\phi$  is close to 1, the whole domain is filled with grains, then if we increase  $\phi$ , the influence is very small. That is why the discrepancy reaches the maximal value at  $\phi = 0.5$  and becomes very small when  $\phi$  is very larger or small. This phenomenon illustrates that the micro-structures of a porous medium can influence the mass diffusion process evidently and the Maxwell equation, which only consider the granular fraction is not exact when  $\phi$  is not very small or larger.

The results for non-permeable grains are shown in Fig. 8b. Unlike in the cases of permeable grains, they are in less agreement with Maxwell equation. The results for various cases are seen to coalesce when the granular fraction is very small, which is like in the cases of permeable grains. However, they start to deviate from one another as  $\phi$  increases. Especially, the case for the staggered square grains deviates early since the flow passage is blocked rapidly when  $\phi$  is close to 0.5. The corresponding concentration fields are presented in Fig. 9. The granular fractions for these two cases are 0.2475, 0.4851 for in-line, and 0.3288, 0.4901 for staggered, respectively. The spaced

**Fig. 8** Effective mass diffusivity for 2D regular media. **a** Permeable grains, **b** non-permeable grains

**Fig. 9** Concentration distribution for 2D regular case. **a** In-line, **b** staggered

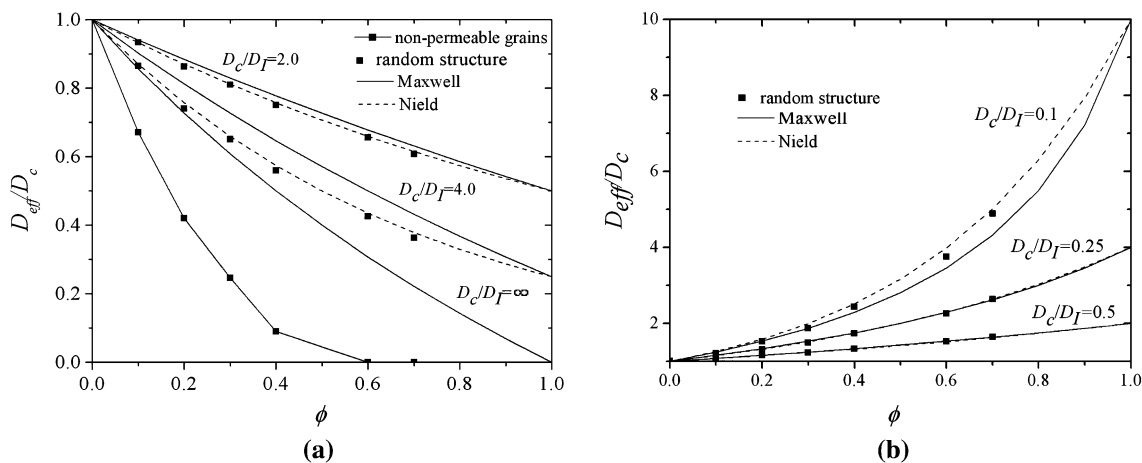
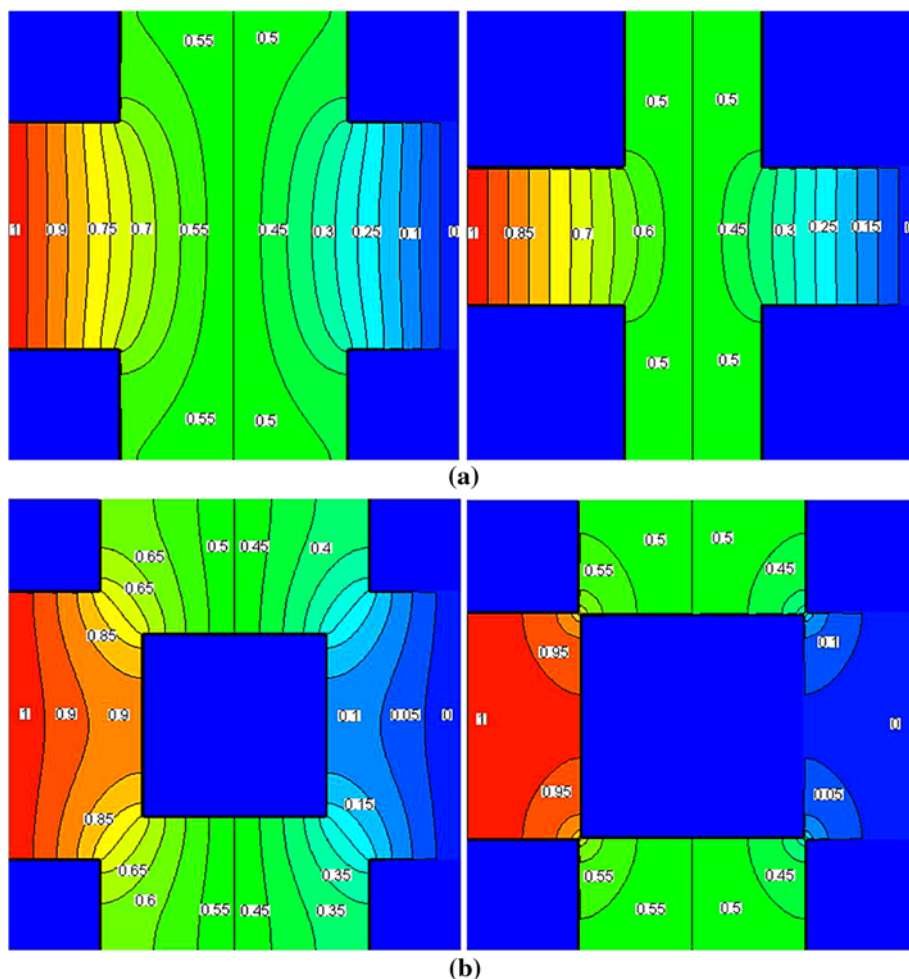


**Fig. 10** Effective mass diffusivity for 2D random media. **a**  $D_c/D_I > 1.0$ , **b**  $D_c/D_I < 1.0$

contours indicate that the concentration varies rapidly as the flow passage becomes narrow for both in-line and staggered case. But for the staggered case, the flow passage decreases very quickly with increasing  $\phi$  and the effective mass diffusivity may deviate sharply from the in-line case as is seen in Fig. 8b.

5.2 2D random porous media

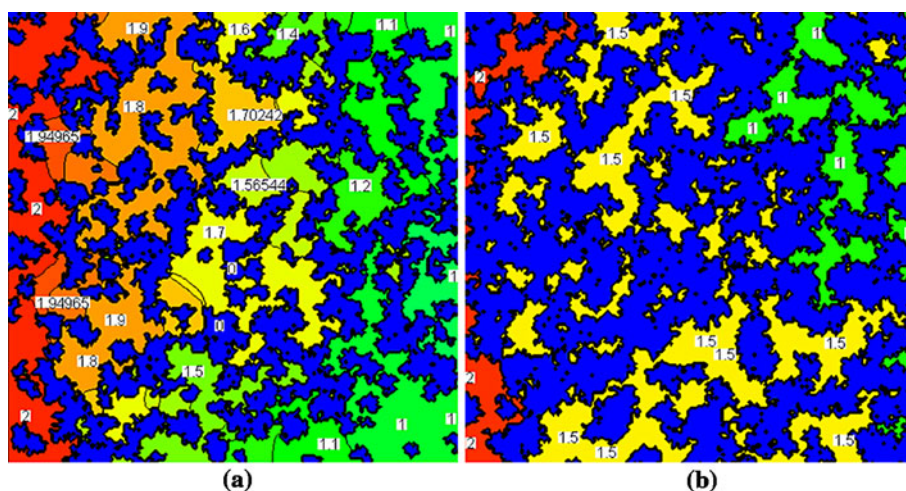
The calculations for 2D random structures are carried out with the same parameters as 2D regular cases above. The cases for  $D_c/D_I > 1$  and  $D_c/D_I < 1$  are both considered in this simulation. The results are shown in Fig. 10.



Unlike in case of regular structure, the results are in much less agreement with Maxwell equation, but much closer to the Nield equation, which indicates that the Nield equation is more applicable for predicting the effective mass diffusivity than the Maxwell equation. This may be attributed to the random effect of grain or pore shape and topological properties. Especially, the results for non-permeable grains ( $D_C/D_I = \infty$ ) decrease much quicker than the case for regular structures. It may indicate that the flow passage is blocked seriously as  $\phi$  increases and when  $\phi$  is close to 0.5, the effective mass diffusivity becomes zero immediately, which is similar to the regular case.

The corresponding concentration fields are shown in Fig. 11. The granular fractions for these two cases are 0.4 and 0.7. The spacial contours indicate that the solid–pore interfaces are treated well with the present bounce-back scheme for non-permeable grains and the flow passage decreases very quickly with increasing  $\phi$ . When the granular fraction is larger than 0.5, the flow passage is blocked completely. So we can predict that for a random porous medium with non-permeable grains, the granular fraction  $\phi = 0.5$  is a critical value for the mass diffusion and the effective mass diffusivity may becomes very small (close to zero) when  $\phi > 0.5$ . This phenomenon can be found in some practical application, such as VOCs problem. According to Ref. [17], for the medium-density board with granular fraction around 53%, the calculated effective mass diffusion coefficient is on the order of  $10^{-11} \text{ m}^2 \text{ s}^{-1}$  and Fick diffusion coefficients of the formaldehyde or the acetaldehyde are on the order of  $10^{-5} \text{ m}^2 \text{ s}^{-1}$ , so for the structure in Ref. [17], the  $D_{eff}/D_c$  is on the order of  $10^{-6}$ , which is very small and consistent with our analysis. Thus, this is encouraging. So the Nield equation is more suitable to estimate the effective mass diffusivities for VOCs problem.

**Fig. 11** Concentration distribution for 2D random cases. **a**  $\phi = 0.4$ , **b**  $\phi = 0.7$



### 5.3 3D random porous media

The effective mass diffusivity for 3D random porous media is very important and practical, because of their similarity to the real porous media. Hence, both the influence of granular fraction and granular diameter are investigated in the following simulation.

#### 5.3.1 Granular fraction effect

In this paper, the cases for  $D_C/D_I > 1$  and  $D_C/D_I < 1$  are also both considered. The results are shown in Fig. 12. The correlations of Maxwell are included in the figure for comparison.

As shown in Fig. 12, when the difference between  $D_C$  and  $D_I$  is small irrespective of their ratio being greater or smaller than 1, the present predictions agree well with Maxwell equation. For  $D_C/D_I > 1$  case, as  $D_C$  becomes much larger than  $D_I$ , Maxwell equation is found to overestimate the effective mass diffusivity, otherwise, as  $D_I$  becomes much larger than  $D_C$ , Maxwell equation is found to underestimate the effective mass diffusivity. One may conclude that Maxwell equation can be used to predict the effective mass diffusivity almost exactly not only for  $D_C/D_I > 1$ , but also for  $D_C/D_I < 1$ , when the difference between  $D_I$  and  $D_C$  as well as the granular fraction  $\phi$  is quite small. But it is found that the calculated results are in much better agreement with Nield equation in the both cases for  $D_C/D_I < 1$  and  $D_C/D_I > 1$ . In the former, Nield equation is found to underestimate the effective mass diffusivity a little, but in the case for  $D_C/D_I > 1$ , it is in good agreement with the calculated data in a porous medium whose constituents have moderately different mass diffusivities. Generally, Nield equation is better than the Maxwell equation to estimate the effective mass diffusivity of a 3D random porous medium. Comparisons with the results for 2D regular media show that the effective mass

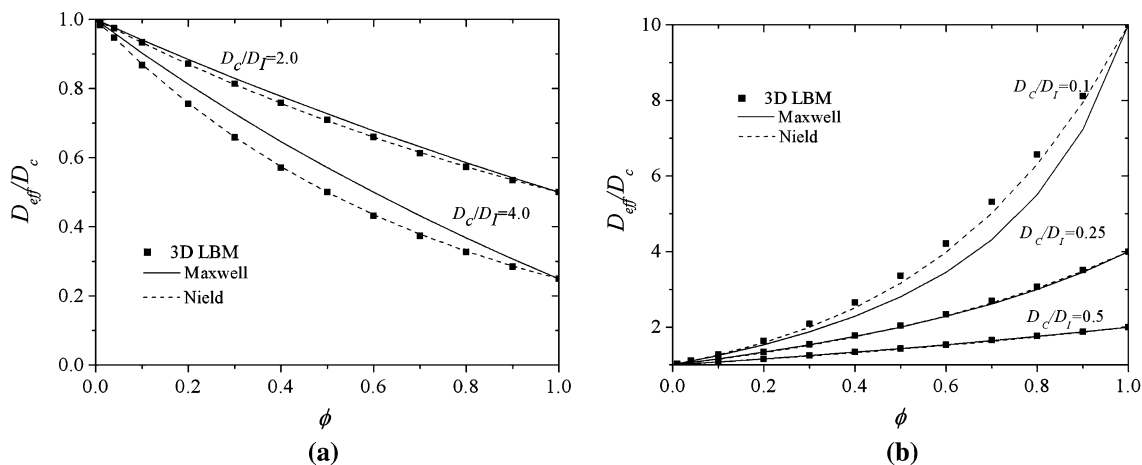


**Fig. 12** Effective mass diffusivity for 3D random media. **a**  $D_c/D_l > 1.0$ , **b**  $D_c/D_l < 1.0$

diffusivity depends considerably on the granular shape, the random volumetric and topological properties such as pore tortuosity and interconnectivity. Hence, Maxwell equation is not quite well for the estimation of the effective mass diffusivity for 3D random porous media.

For  $D_c/D_l < 1$ , the existing equations are found to underestimate the effective mass diffusivity, so a new empirical correlation is obtained by using a quadratic polynomial as following:

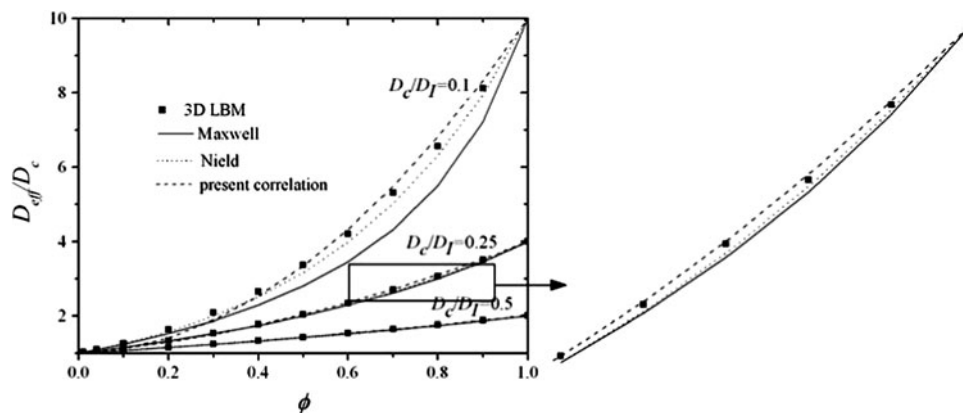
$$\frac{D_{eff}}{D_c} = c_0 + c_1\phi + c_2\phi^2. \tag{22}$$

When  $\phi = 0$  and  $1$ , the corresponding  $\frac{D_{eff}}{D_c}$  is  $1$  and  $\frac{D_l}{D_c}$ , respectively. We can obtain that  $c_0 = 1.0$  and  $c_1 + c_2 = \frac{D_l}{D_c} - 1$ . Considering the influence of the ratio of the two diffusivities and fitting the data of Fig. 12b in a least-squares sense,  $c_1$  and  $c_2$  are finally determined as

$$a_1 = -0.019 + 0.4598\frac{D_l}{D_c} - 0.0421\left(\frac{D_l}{D_c}\right)^2 \tag{23}$$

$$a_2 = -0.981 + 0.5402\frac{D_l}{D_c} + 0.0421\left(\frac{D_l}{D_c}\right)^2. \tag{24}$$

**Fig. 13** Comparisons among the resent correlation, Maxwell equation, Nield equation, and the data of LBM



Comparisons between the above correlation and the results for 3D random porous medium are shown in Fig. 13. The correlation is in better agreement with the data of 3D random porous medium and when the difference between  $D_c$  and  $D_l$  becomes larger, the data of 3D random porous medium are located between the present correlation and the Nield’s equation, yet closer to our new correlation.

The concentration field, where the concentration equals 0.3 inside the porous media with two different porosities at  $D_c/D_l = 0.1$  is shown in Fig. 14. The results show that because of the micro-structure of the porous medium, the surfaces are rough and as  $\phi$  increases, they become more smooth. It indicates that the influence of the pore or granular structure is considered in our LBM model.

5.3.2 Granular diameter effect

Figure 15 shows the calculated effective mass diffusivity versus the average characteristic diameter of solid particles, which is defined as the sphere diameter of the average volume of a particle. For the QSGS method, the average

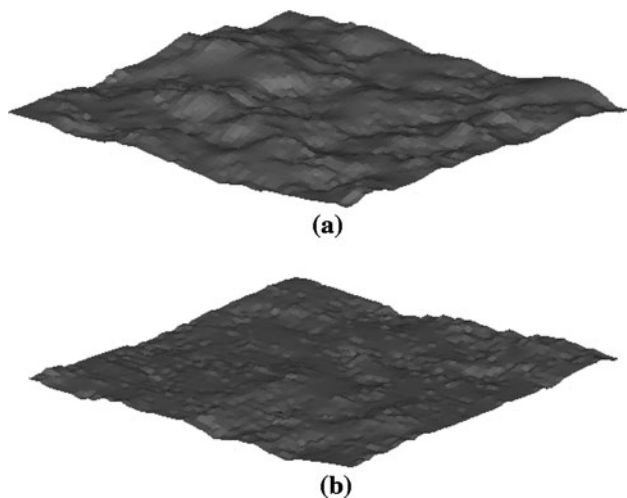


**Fig. 14** The surfaces inside the 3D random media with an equal concentration ( $C = 0.3$ ). **a**  $\phi = 0.3$ , **b**  $\phi = 0.9$

volume of a particle is calculated by the following equation [28].

$$V_p = (1 - \varepsilon)V/(\eta \cdot C_d) \tag{25}$$

where  $V$  represents the total volume of the system,  $\eta$  is the total grid number, and  $C_d$  is the core distribution probability.

Without losing universality, we introduce a dimensionless average characteristic diameter  $\lambda$ , which can be related to the average characteristic diameter  $d$  as  $\lambda = d/d_x$ , where  $d_x$  is defined as  $d_x = L/M$ , where  $L$  represents the length of the reconstruction system,  $M$  the grid number in one direction.

From above we obtain that

$$\frac{1}{6}\pi(\lambda d_x)^3 = (1 - \varepsilon)V/(\eta \cdot C_d) \tag{26}$$

Finally, from Eqs. 25 and 26, the dimensionless characteristic diameter  $\lambda$  can be related to  $C_d$  as

$C_d = \frac{6(1-\varepsilon)}{\pi\lambda^3} \approx \frac{1.9099(1-\varepsilon)}{\lambda^3}$ . Considering the constraint that  $C_d < (1 - \varepsilon)$ , the lower limit of  $\lambda$  is 1.24 (i.e.,  $\lambda > 1.24$ ).

Here, the dimensionless average characteristic diameter changes from 1.5 to 9.3 by varying  $C_d$  from 0.3395 to 0.0014 in the present simulations and other parameter is  $\varepsilon = 0.4$ . The cases for  $D_c/D_l > 1$  and  $D_c/D_l < 1$  are also both considered. The results show that whether  $D_c/D_l > 1$  or  $D_c/D_l < 1$ , when the difference between  $D_c$  and  $D_l$  is small irrespective of their ratio being greater or smaller than 1, the change of the effective mass diffusivity for 3D random structure versus the average characteristic diameter of solid particles is very small, but when the difference increases, the effective mass diffusivity increases evidently as  $\lambda$  increases. Comparing Fig. 15a with Fig. 15b, we can conclude that the rate of the effective mass diffusivity increasing with the average characteristic diameter in the case for  $D_c/D_l > 1$  is smaller than the case for  $D_c/D_l < 1$ . Because of the stochastic characteristics for the 3D random porous medium, two trials were performed for each dimensionless average characteristic diameter, but the calculated effective mass diffusivities did not exactly fall into a same value. For a given porous medium and a  $D_c/D_l$ , a smaller dimensionless average characteristic diameter leads to a smaller fluctuation around the average result. Furthermore, these statistic fluctuations increases evidently, when the difference between  $D_c$  and  $D_l$  increases. For the present simulations in Fig. 15, the statistical fluctuation is smaller than 4%.

### 6 Conclusions

In this paper, the effective mass diffusivity through the porous medium is successfully predicted by the lattice Boltzmann method. The results that have been obtained for various 2D and 3D structures are compared with the

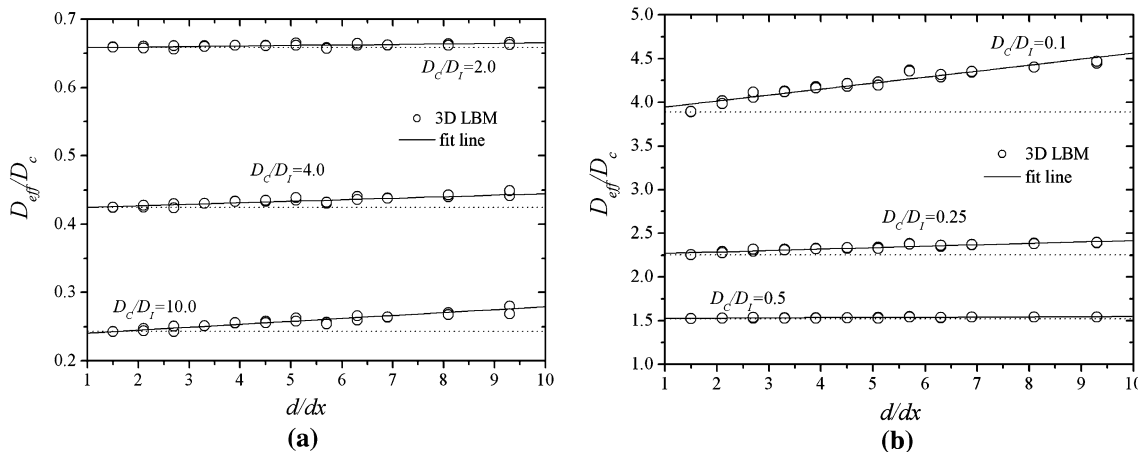


**Fig. 15** The effective mass diffusivity versus average characteristic diameter of solid particles. **a**  $D_c/D_l > 1.0$ , **b**  $D_c/D_l < 1.0$

existing analytic equations. The results, generally, are in good agreement with the existing analytical equation of Maxwell equation and Nield equation in some specially situation. The Maxwell equation is suitable for 2D regular, 2D random and 3D random porous medium for permeable grains, whose diffusivity is not much different from that of the species inside the pores. When the difference between the diffusivity of grains and fluid becomes larger, the Maxwell equation is not applicable and for the 3D random medium, the effect of the grain or pore shape, the random volumetric and topological properties such as pore tortuosity and interconnectivity becomes significant and the results deviate rather sharply from Maxwell equation. But the Nield equation seems much more comprehensive. Especially, for a 3D random porous medium, the results calculated by the Nield equation are much closer to our present data. Thus, for the VOCs problem, Nield equation can be used to evaluate the effective mass diffusivity. Furthermore, for non-permeable grains with moderate granular fraction, the analytical solution of Maxwell is not adequate in estimating the effective mass diffusivity well. This may be due to that the flow passage becomes narrow and decreases very quickly with increasing granular fraction and this may be very serious for 2D random medium.

Generally, the present full numerical set is quite suitable for analyses of mass diffusion in the porous media. The results and methodology in this contribution may be of great significance for improving our understandings of mass transport mechanisms in various porous media. Yet, it can provide some meaningful data and theoretical analysis to some practice application, such as the VOCs. According to our results above, we can know the influence of the granular fraction, random structures, random granular shape and the average granular diameter on the mass diffusion in a porous media, which can guide us to control volatilization of the organic compounds in VOCs problem. Future work will focus on the influence of the thermal effect on the mass diffusion inside a porous medium.

**Acknowledgments** This study was supported by National Natural Science Foundation of China (Grant nos. 50478012, 50725620). The authors would like to thank the helpful discussions from Dr. J. Y. Xiong, and Prof. Y. P. Zhang about the VOCs problem. A special thanks is also given to Dr. Wang for his patient and useful discussions on the QSGS method.

## References

- Cao Y, Faghri A (1994) Analytical solutions of flow and heat transfer in a porous structure with partial heating and evaporation on the upper surface. *Int J Heat Mass Transf* 36(10):1525–1533
- Cao Y, Faghri A (1994) Conjugate analysis of a flat-plate type evaporator for capillary pumped loop with three-dimensional vapor flow in the groove. *Int J Heat Mass Transf* 37(3):401–409
- Tarik K, John G (2006) Numerical analysis of heat and mass transfer in the capillary structure of a loop heat pipe. *Int J Heat Mass Transf* 49:3211–3220
- Ren C, Wu QS, Hu MB (2007) Heat transfer with flow and evaporation in loop heat pipe's wick at low or moderate heat fluxes. *Int J Heat Mass Transf* 50:2296–2308
- Qian JY, Li Q, Xuan YM (2004) A novel method to determine effective thermal conductivity of porous material. *Sci Chin Ser E Technol Sci* 47:716–724
- Bhattacharya A, Calmidi VV, Mahajan RL (2002) Thermophysical properties of high porosity metal foams. *Int J Heat Mass Transf* 45(5):1017–1031
- Paek JW, Kang BH, Kim SY, Hyun JM (2000) Effective thermal conductivity and permeability of aluminum foam materials. *Int J Thermophys* 21(2):453–464
- Manwart C, Aaltosalmi U, Koponen A, Hilfer R, Timonen J (2002) Lattice-Boltzmann and finite-difference simulations for the permeability for three-dimensional porous media. *Phys Rev E* 66(1):016702/1–11
- Kim YM, Harrad S, Harrison RM (2001) Concentrations and sources of VOCs in urban domestic and public microenvironments environ. *Sci Technol* 35:997–1004
- Meininghaus R, Salthammer T, Knoppel H (1999) Interaction of volatile organic compounds with indoor materials—a small-scale screening method. *Atmos Environ* 33:2395–2401
- Molhave L (1989) Sick buildings and other buildings with indoor climate problems. *Environment* 15:473–482
- Cox SS, Zhao D, Little JC (2001) Measuring partition and diffusion coefficients for volatile organic compounds in vinyl flooring. *Atmos Environ* 35:709–714
- Haghighat F, Zhang Y (1999) Modeling of emission of volatile organic compounds from building materials—estimation of gas-phase mass transfer coefficient. *Build Environ* 37:1349–1360
- Lee CS, Haghighat F, Ghaly WS (2005) A study on VOC source and sink behavior in porous building materials—analytical model development and assessment. *Indoor Air* 15:183–196
- Little JC, Hodgson AT, Gadgil AJ (1994) Modeling emissions of volatile organic compounds from new carpets. *Environment* 28:227–234
- Hu HP, Zhang YP, Wang XK, Little JC (2007) An analytical mass transfer model for predicting VOC emissions from multi-layered building materials with convective surface on both sides. *Int J Heat Mass Transf* 50:2069–2077
- Xiong JY, Zhang YP, Wang XK, Chang DW (2008) Macro-meso two scale model for predicting the VOC diffusion coefficients and emission characteristics of porous building materials. *Atmos Environ* 42:5278–5290
- Frank PI, David PD (2002) *Fundamentals of heat and mass transfer*, 5th edn. Wiley, New York, pp 859–870
- Benzi R, Succi S, Vergassola M (1992) The lattice-Boltzmann equation: theory and applications. *Phys Rep* 222:145–197
- Qian Y, Succi S, Orszag S (1995) Recent advances in lattice Boltzmann computing. *Annu Rev Comp Phys* 3:195–242
- Chen S, Doolen GD (1998) Lattice Boltzmann method for fluid flows. *Annu Rev Fluid Mech* 30:329–364
- Xuan YM, Li Q, Ye M (2007) Investigations of convective heat transfer in ferrofluid microflows using lattice-Boltzmann approach. *Int J Therm Sci* 46:105–111
- Li HN, Pan CX, Miller CT (2005) Pore-scale investigation of viscous coupling effects for two-phase flow in porous media. *Phys Rev E* 72:026705/1–14
- Li Q, Zheng CG, Wang NC, Shi BC (2001) LBGK simulations of Turing patterns in CIMA model. *J Sci Comput* 16:121–134
- Toffoli T, Margolus N (1990) Invertible cellular automata: a review. *Physica D* 45:229–253

26. Kang QJ, Zhang DX, Lichtner PC, Tsimpanogiannis IN (2004) Lattice Boltzmann model for crystal growth from supersaturated solution. *Res Lett* 31:L21604
27. Wang J, Wang M, Li Z (2007) A lattice Boltzmann algorithm for fluid–solid conjugate heat transfer. *Int J Therm Sci* 46:228–234
28. Wang M, Chen SY (2007) Electroosmosis in homogeneously charged micro- and nano-scale random porous media. *J Colloid Interface Sci* 314:264–273
29. Jose AR, Salvador NM, Jesús GT (1996) Calculation of the effective diffusivity of heterogeneous media using the lattice-Boltzmann method. *Phys Rev E* 53:2298–2303
30. Maxwell JC (1954) *A treatise on electricity and magnetism*, 3rd edn. Dover, New York
31. Nield DA (1991) Estimation of the stagnant thermal conductivity of saturated porous media. *Int J Heat Mass Transf* 34:1575–1576
32. Guo ZL, Shi BC, Zheng CG (2002) A coupled lattice BGK model for Boussinesq equations. *Int J Numer Methods Fluids* 39:325–342
33. Zhao K, Li Q, Xuan YM (2009) Investigation on the three-dimensional multiphase conjugate conduction problem inside porous wick with the lattice Boltzmann method. *Sci Chin Ser E Technol Sci* 52(10):2973–2980
34. Shi MH, Li XC (2006) Determination of effective thermal conductivity for polyurethane foam by use of fractal method. *Sci Chin Ser E Technol Sci* 49:468–475